JOURNAL OF MATERIALS SCIENCE 35 (2000) 4159–4164

Crystallization behavior of $Ti_{50}Ni_{25}Cu_{25}$ amorphous alloy

D. V. LOUZGUINE, A. INOUE
Institute for Materials Research, Tohoku University, Katahira 2-1-1, Aoba-Ku, Sendai 980-8577, Japan
E-mail: dmluz@imrtuns.imr.tohoku.ac.jp

Crystallization behavior of the $Ti_{50}Ni_{25}Cu_{25}$ alloy was studied by means of scanning and isothermal differential calorimetry, X-ray diffraction, conventional and high-resolution transmission electron microscopy. A single stage polymorphic-type transformation of the amorphous phase forming a Ti_2CuNi crystalline phase was observed. The activation energy for such a single stage crystallization of the amorphous phase was determined by Kissinger analysis. Kinetics of the crystallization was analyzed on the basis of Johnson-Mehl-Avrami equation and discussed regarding to the value of Avrami exponent obtained. Relatively high average value of Avrami exponent of 5.5 at the range from 702 to 709 K suggests nucleation with an increasing nucleation rate.

1. Introduction

Ti-based amorphous alloys are of significant interest as they have high tensile strength exceeding 1500 MPa, for example 1800 MPa [1], in the case of recently studied [2] $Ti_{50}Ni_{25}Cu_{25}$ alloy. Relatively low density of the main alloying element Ti of 4500 kg/m^3 suggests higher strength/density ratio compare to Fe-or Zr-based amorphous alloys. Moreover, the above-mentioned alloy has high glass-forming ability and can be produced in a bulk form by mold casting [1]. $Ti_{50}Ni_{25}Cu_{25}$ alloy also exhibits glass transition before crystallization and a relatively wide supercooled liquid region of 40 K was observed during differential scanning calorimetry (DSC) carried out at the heating rate of 0.67 K/s [1]. It has been also shown that this alloy crystallizes through a single stage transformation reaction [1, 2].

The purpose of the present study is the crystallization behavior of the $Ti_{50}Ni_{25}Cu_{25}$ alloy. Kinetics of the crystallization was studied in the present work through the use of Johnson-Mehl-Avrami isothermal analysis. An activation energy for the transformation was evaluated by application of Kissinger analysis [3].

2. Experimental procedure

An ingot of the $Ti_{50}Ni_{25}Cu_{25}$ alloy was prepared by arc-melting the mixture of Ti 99.95 mass% purity, Ni 99.9 mass% purity and Cu 99.99 mass% purity in an argon atmosphere. From this alloy, ribbon samples of about 0.02 mm in thickness and 0.9 mm in width were prepared by rapid solidification of the melt on a single copper roller at the wheel surface velocity of 41.9 m/s. The structure of ribbon samples was examined by X-ray diffraction with monochromatic Cu K_α radiation. Transmission electron microscopy (TEM) was carried out using a JEM 2010 microscope operating at 200 kV equipped with energy dispersive X-ray spectrometer. Crystallization temperature and heat of crystallization were examined by differential scanning calorimetry at heating rates ranged from 0.033 to 1.333 K/s. Isothermal calorimetry traces were obtained at the temperature range from 702 to 709 K. The specimens were heated up to testing temperature at 1.667 K/s. Isothermal annealing at 800 and 990 K was carried out in vacuum of $1*10^{-5}$ Torr.

3. Results

3.1. Differential scanning and isothermal calorimetry measurements

The results of differential scanning calorimetry carried out at different heating rates shown in Fig. 1 indicated that the $Ti_{50}Ni_{25}Cu_{25}$ alloy transformed to crystalline state through a single stage exothermic reaction. It should be mentioned that the value of endothermic heat effect related to appearance of supercooled liquid became lower at lower heating rate used in relation with the value of exothermic one that was related to crystallization of the amorphous phase. After completion of the single heat effect the structure was found to be fully crystallized.

Crystallization temperature decreased with decreasing heating rate. The temperature at which the maximum deflection is observed varied with heating rate in the same way. Thus, the kinetic constant can be obtained directly from the DSC data. The activation energy E (the energy barrier opposing the crystallization) in the equation for the fraction transformed x [3]:

$$dx/dt = A(1-x)\exp(-E/RT) \qquad (1)$$

can be obtained directly from the temperature T_m (peak temperature) at which the ratio dx/dt attains the

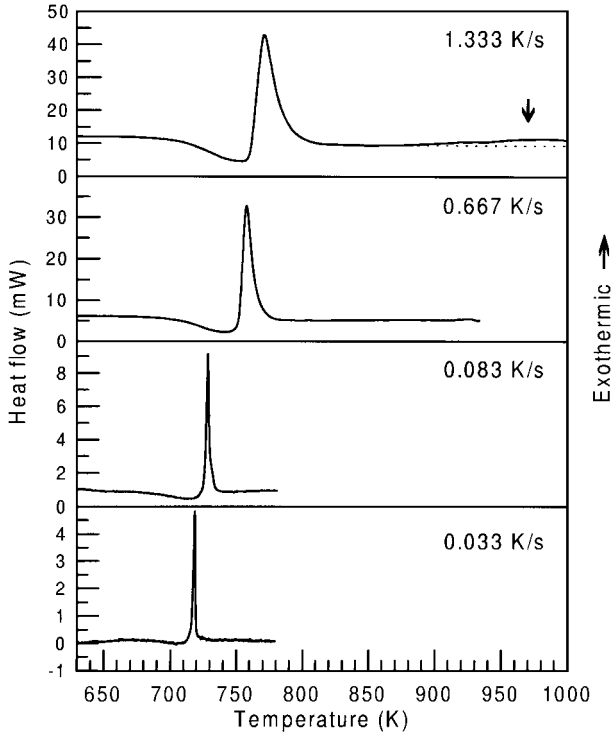

Figure 1 DSC curves taken at different heating rates.

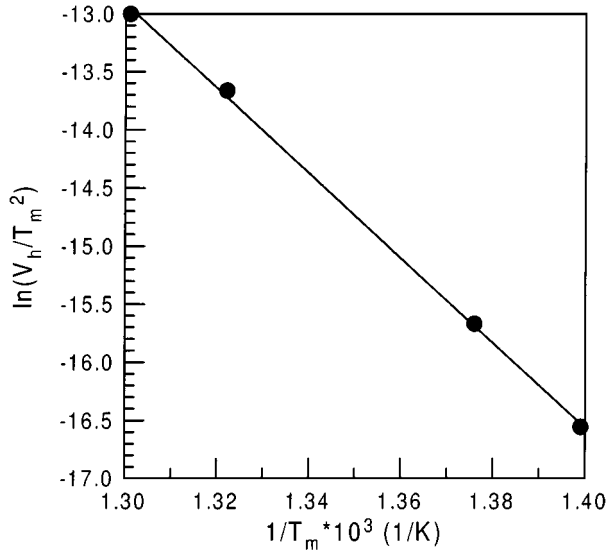

Figure 2 Kissinger plot.

maximum. The corresponding equation is:

$$-E/R = \mathrm{d}\left(\ln V_\mathrm{h}/T_\mathrm{m}^2\right)/\mathrm{d}(1/T_\mathrm{m}) \qquad (2)$$

where V_h is the heating rate and R is the gas constant. The data plotted as indicated by Equation 2, that is to say $(\ln V_\mathrm{h}/T_\mathrm{m}^2)$ vs. $(1/T_\mathrm{m})$ are shown in Fig. 2. From the slope, the activation energy was estimated to be 306 kJ/mol.

The study of the kinetics of crystallization was performed using the Johnson-Mehl-Avrami isothermal analysis for volume fraction x transformed as a function of time t on the basis of the following equation [4]:

$$x(t) = 1 - \exp[-(kt)^n] \qquad (3)$$

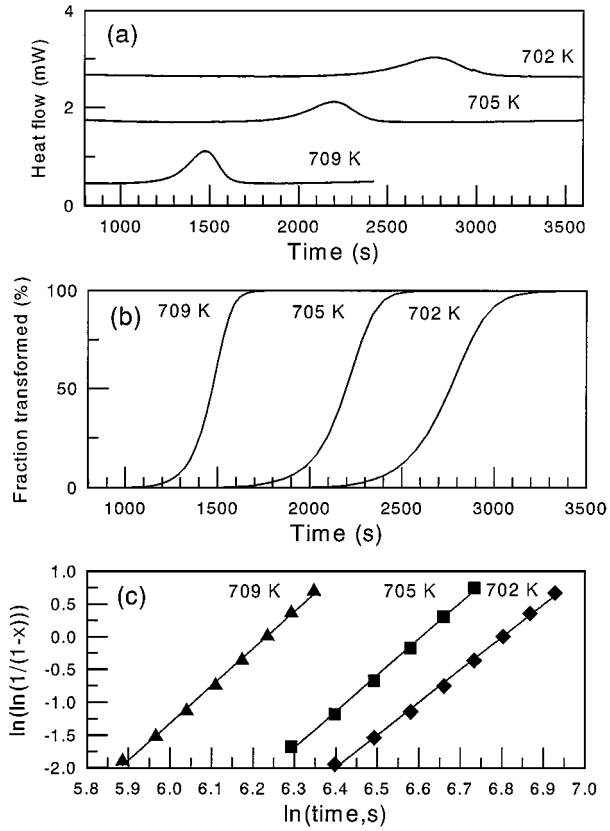

Figure 3 (a) Isothermal differential calorimetry curves, (b) the fraction transformed versus the annealing time, and (c) the Avrami plot.

The samples were annealed isothermally at several temperatures namely 702, 705 and 709 K (see Fig. 3a). The plots are shifted in the Y-axis direction not to intersect each other. The volume fraction transformed versus the annealing time plot is shown in Fig. 3b. The volume fraction transformed at the time t is assumed to scale with the fraction of the total heart released. Equation 3 can be written as:

$$\ln[\ln(1/(1-x))] = n\ln(k) + n\ln(t) \qquad (4)$$

where k is an effective rate constant and n is Avrami exponent. The Avrami plot of $\ln[-\ln(1-x)]$ vs. $\ln(t)$ yields a strait line with slope n and intercept $n\ln(k)$. Fig. 3c shows this plot at three different temperatures. The plots are reasonably linear. The value of Avrami exponent n increases with annealing temperature being 5.1 at 702 K, 5.7 at 705 K and 5.8 at 709 K.

3.2. TEM and X-ray diffraction results

Fig. 4 shows X-ray diffraction patterns of the $Ti_{50}Ni_{25}Cu_{25}$ alloy after DSC up to 780 K carried out at the heating rate of 0.67 K/s (a), and after isothermal annealing for 0.25 (b). 24 (c) and 1 (d) hour at 780, 800 and 990 K, respectively. Peaks marked by (▼) (see Fig. 4) were produced by Ti_2NiCu phase discussed below. Some of the diffraction peaks shown in Fig. 4 belonged to a stable γ CuTi phase, P4/nmm space group, with a tetragonal structure of $a = 0.3108$ nm and $c = 0.5887$ nm [5], some other belonged to another stable $TiNi_{0.8}Cu_{0.2}$ phase having a monoclinic structure of $a = 0.2896$ nm, $b = 0.4239$ nm, $c = 0.4524$ nm and $\beta = 90.016^\circ$ [6]. Several peaks remained unidentified.

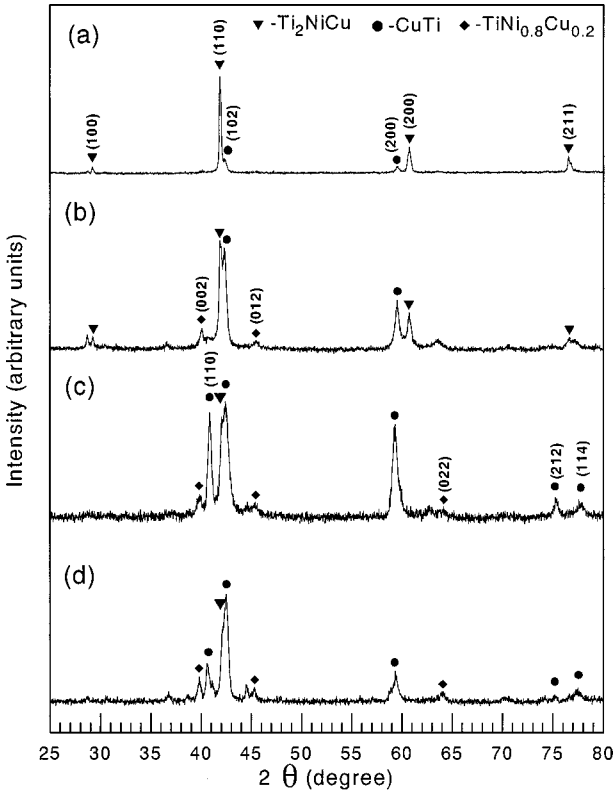

Figure 4 X-ray diffraction patterns of the $Ti_{50}Ni_{25}Cu_{25}$ alloy after DSC up to 780 K at the heating rate used of 0.67 K/s (a), and after isothermal annealing for 0.25 (b), 24 (c) and 1 (d) hour at 780, 800 and 990 K, respectively.

TEM results of the sample annealed isothermally in calorimeter at 709 K for 1680 s just up to the completion of the exothermic reaction are shown in Fig. 5. As seen in Fig. 3a at this stage crystallization is almost completed. Fig. 5a shows that the structure consists of faceted crystals of a compact shape of about 300–900 nm in size. High-resolution TEM image (Fig. 5b) taken from the single particle confirmed that these particles are single crystals. A group of crystalline particles is shown in Fig. 5c, d. Three selected-area electron diffraction patterns obtained from the crystalline particles (see Fig. 5c, d) are shown in Fig. 5e–g. By the EDX analysis an average composition of the crystalline phase was found to be 49 at% Ti, 25 at% Ni and 26 at% Cu that is very close to the composition of the amorphous alloy. Thus, the composition of such a ternary phase could be written as Ti_2NiCu. Its chemical composition slightly changed form particle to particle suggesting formation of solid solutions.

Decomposition of the Ti_2NiCu phase starts right after the completion of the strong exothermic reaction (see Fig. 1) from precipitation of γ CuTi phase (see Fig. 4a). The structure of the sample annealed for 1 h (3600 s) at 990 K is shown in Fig. 6. The size of faceted particles of the ternary Ti_2NiCu phase is almost the same as shown in Fig. 5, however plate-shaped crystals of γ CuTi phase appeared to form from the Ti_2NiCu phase as shown in the dark field image (Fig. 6d) taken in the reflection N: 2 of Fig. 6a. Diffraction pattern shown in Fig. 6a contains reflections from both phases. The section of the reciprocal lattice formed by the strong (indexed) spots in Fig. 6a corresponds to the Ti_2NiCu phase. A very weak prolonged heat effect marked by arrow in Fig. 1 could be responsible for the decomposition of the ternary phase with the formation of γ CuTi phase. Chemical composition of the plate-shaped crystal of γ CuTi phase (Fig. 6d) was found to be 45.5 at% Ti, 7.7 at% Ni and 46.8 at% Cu that is probably a solution of Ni in γ CuTi phase. If Ni is not taken into consideration during calculation, the composition, the composition will be very close to nominal composition of the CuTi phase, namely 49.3 at% Ti and 50.7 at% Cu. EDX spectrums were taken at different electron beam size ranged from 2 to 10 nm depending on the particle size. EDX spectrums taken from both phases (see Fig. 6c, d) are shown in Fig. 7. The composition of the Ti_2NiCu particle (see Fig. 6c) was 44.0 at% Ti, 31.2 at% Ni and 24.8 at% Cu. It should be noticed, that even after a relatively long term (3600 s) annealing at the temperature of 990 K a large volume fraction of the Ti_2NiCu phase existed in the structure. Only some of Ti_2NiCu particles undergo transoformation and the average chemical composition of the particles of ternary Ti_2NiCu phase is 45 at% Ti, 28 at% Ni and 27 at% Cu. The particle of the ternary phase shown in Fig. 6 is enriched in Ni compare to other particles that did not undergo transformation yet. $TiNi_{0.8}Cu_{0.2}$ and an unidentified phased were formed after CuTi.

4. Discussion

As has been pointed out, the value of endothermic heat effect related to appearance of supercooled liquid become lower at lower heating rate used in relation with the value of exothermic one related to crystallization of the amorphous phase (see Fig. 1). Almost no glass transition is seen at the heating rate of 0.033 K/s due to structural relaxation during slow heating. Thus, glass transition in $Ti_{50}Ni_{25}Cu_{25}$ alloy is greatly sensitive to the heating rate.

$Ti_{50}Ni_{25}Cu_{25}$ alloy crystallizes through a single stage polymorphic reaction forming a Ti_2NiCu phase. High average value of Avrami exponent of 5.5 at the range from 702 to 709 K suggests nucleation with an increasing nucleation rate. Moreover, an increase of the value of Avrami exponent with annealing temperature illustrates that nucleation rate is thermally activated process. The activation energy of 306 kJ/mol is close to that 345 kJ/mol for polymorphic crystallization of binary Ti_2Ni alloy studied earlier [7].

Diffraction patterns taken from the particles of ternary Ti_2NiCu phase showed a high symmetry of this phase (see Fig. 5). The location of some diffraction lines produced by Ti_2NiCu phase are close to that of the binary CuTi phase (see Fig. 4). According to the indexing of the diffraction patterns shown in Fig. 5e–g the Ti_2NiCu phase was found to have a cubic lattice with a lattice parameter $a = 0.3047$ nm. It is hard to obtain this value more precisely as highly-indexed (220) peak is broad and has a low intensity. Experimental and calculated angles between crystallographic planes according to the sections [100] [111] and [110] of reciprocal lattice Fig. 5e–g, respectively, are summarized in Table I. Although the Ti_2NiCu particles are quite large (300–900 nm in size) the diffraction lines in Fig. 4 are

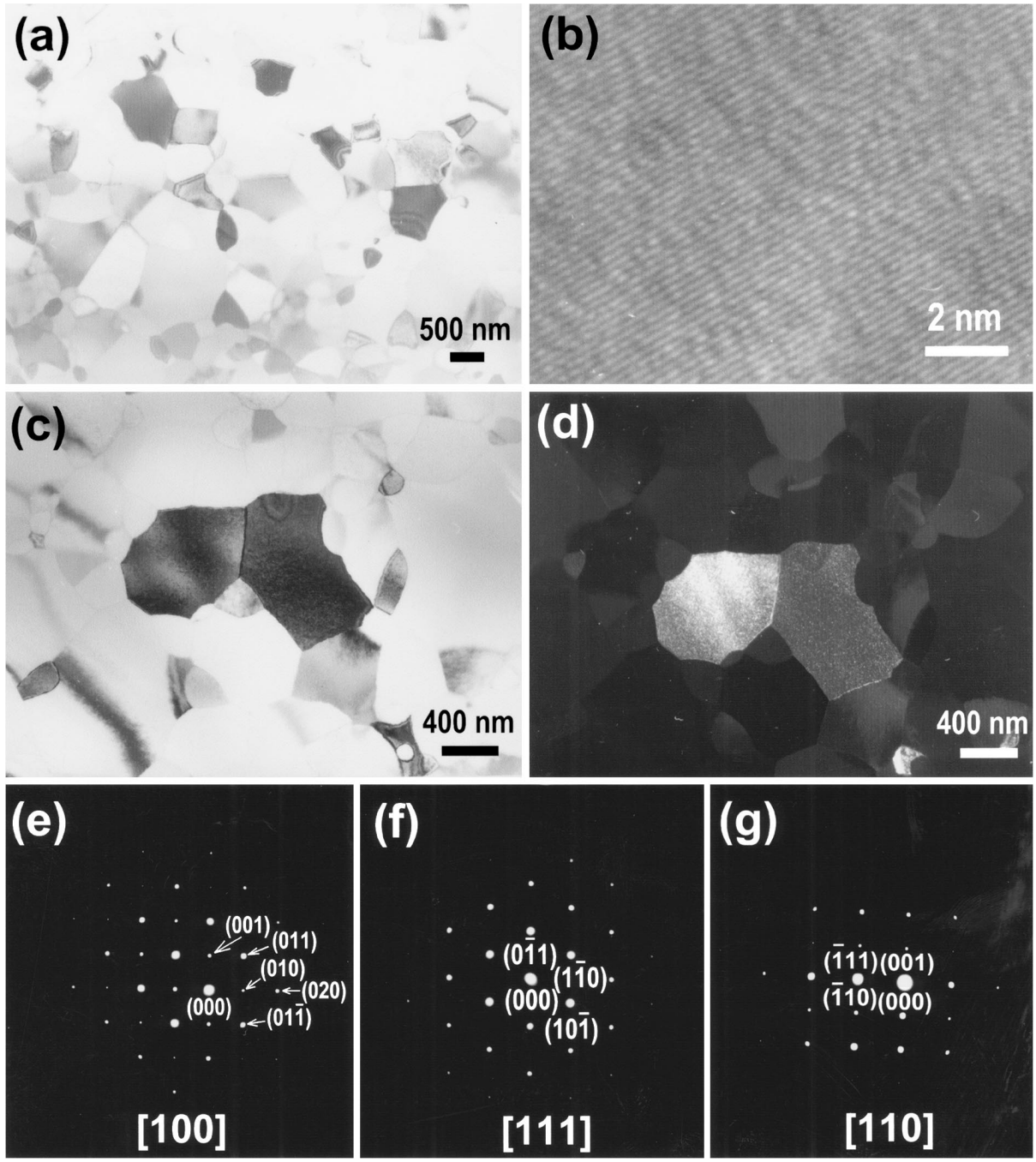

Figure 5 (a) Microstructure of $Ti_{50}Ni_{25}Cu_{25}$ alloy, bright-field image. (b) High-resolution transmission electron microscopy, (c) bright- and (d) dark-field images of a group of particles, respectively. (e), (f) and (g) - selected area electron diffraction patterns. The sample heat treated for 1680 s at 709 K.

TABLE I Experimental and calculated d-spacings and angles between some crystallographic planes in a cubic lattice with a lattice parameter $a = 0.3047$ nm according to selected-area diffraction patterns shown in Fig. 5e–g

Zone axis [uvw]	Plane 1 $h_1k_1l_1$	Plane 2 $h_2k_2l_2$	Angle between to planes, degree	
			Experimental	Calculated
[100]	(011)	(01−1)	90	90
	(011)	(002)	45	45
[111]	(0−11)	(1−10)	60	60
	(1−10)	(10−1)	60	60
[110]	(−111)	(001)	55	54.7
	(−110)	(−111)	35	35.3

broad suggesting high degree of microdeformation. The d-spacings corresponding to different diffraction peaks and the relative intensities of those peaks obtained from the X-ray diffraction pattern shown in Fig. 4a are summarized in Table II together with the values calculated according to the unit cell. The lattice parameter of Ti_2NiCu is very close to that of the Pm 3m cubic NiTi phase that allows us to suppose that this phase is a solid solution of Cu in NiTi phase.

Taking into account chemical composition of Ti_2NiCu phase one can suppose that Cu atom replace Ni atoms located at the corners of the unit cube.

Chemical composition of the Ti_2NiCu phase slightly changes form particle to particle suggesting formation

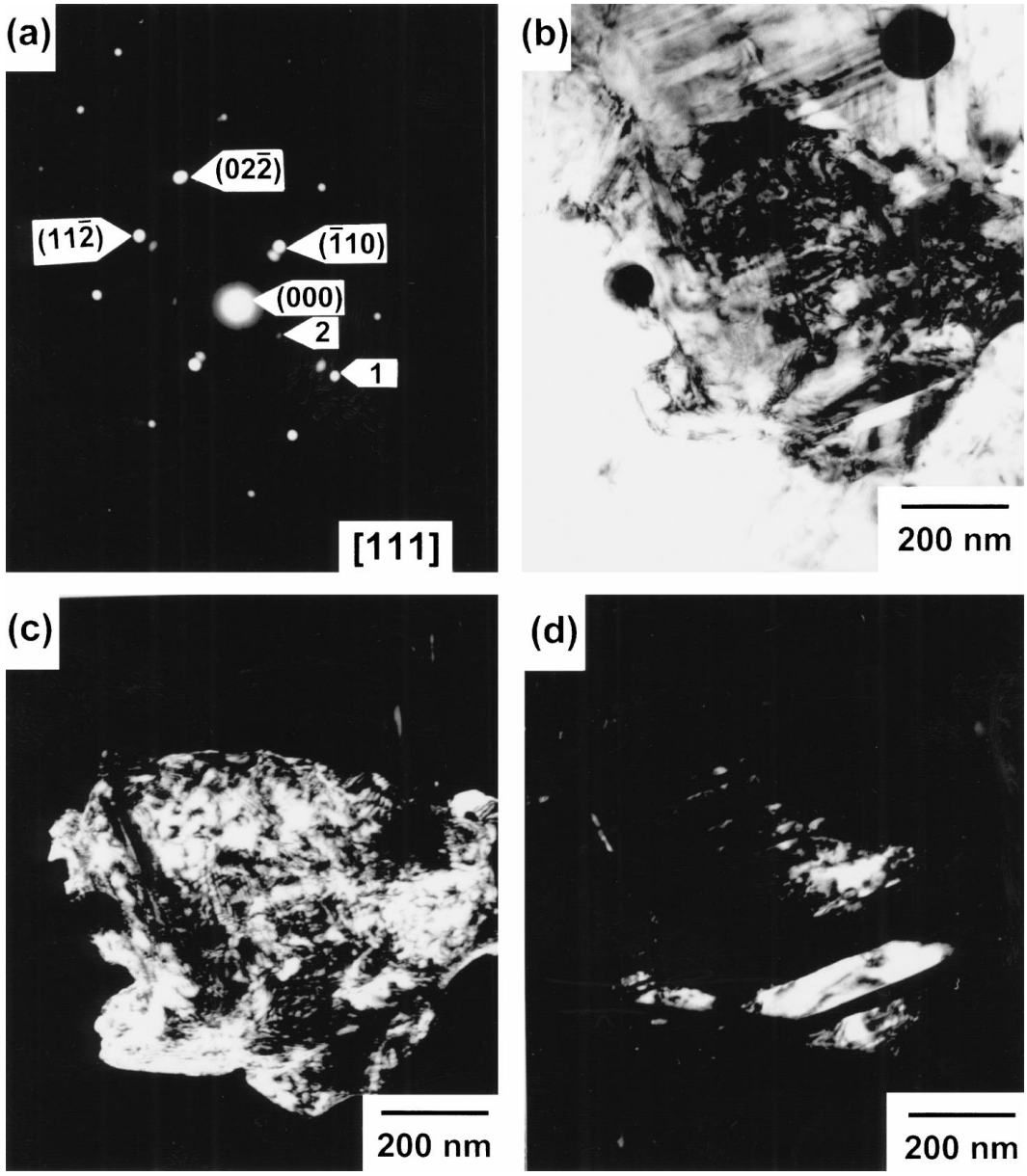

Figure 6 (a) Selected area electron diffraction pattern, (b) bright-field and (c) and (d) dark-field images respectively taken from the reflections 1 and 2, respectively marked by arrows in the pattern (a). The sample heat treated for 1 hour (3600 s) at 990 K.

TABLE II Experimental and calculated *d*-spacings and experimental relative intensities for the Ti_2NiCu phase discussed in the text

d-spacings, nm		Relative integrated intensities		
Experimental	Calculated	Experimental	Calculated	*HKL*
0.3051	0.3047	4	0	(100)
0.2155	0.2155	100	100	(110)
0.1525	0.1524	22	12	(200)
0.1243	0.1244	17	18	(211)
0.1076	0.1077	4	5	(220)

of solid solutions. γ CuTi phase also has a definite area of homogeneity on the phase diagram of the Ti-Cu-Ni system [8] in expense of dissolution of Ni. Replacement of 25 at% Cu by Ni in the CuTi phase gives the composition of the above-mentioned ternary phase that can be accompanied by the change in atomic positions and in the crystalline symmetry.

The transformation of Ti_2NiCu phase into CuTi one begins just after the completion of the crystallization. After DSC up to 780 K the lines of CuTi phase are already seen in the X-ray diffraction pattern (Fig. 4a). During solid state phase transformation Ti_2NiCu phase is gradually depleting in Ti and Cu.

Although at the offset of the single stage crystallization the crystalline particles of the ternary phase are as large as about 300–900 nm they are relatively stable against growth or coalescence at higher temperature. No significant change in those size or morphology is seen (Fig. 6) in micrographs of the sample annealed for 3600 s at 990 K. Thus, Ti_2NiCu phase being metastable shows high thermal stability. The process of the decomposition of the ternary phase goes relatively slowly even at the temperature as high as 990 K that is close to the melting temperature of the alloy of about 1050 K. As has been pointed out not all of grains of the ternary phase undergo transformation during annealing for 3600 s at 990 K.

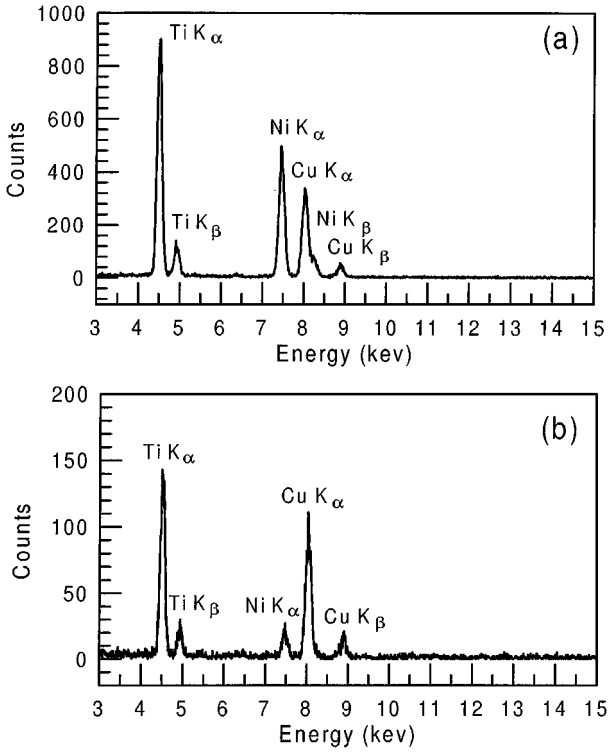

Figure 7 EDX spectrums taken (a) from the polyhedral phase (see Fig. 6c) and (b) plate-shaped precipitate (see Fig. 6d). Beam size 10 nm and 2 nm, respectively. The sample heat treated for 1 hour at 990 K.

5. Conclusions

$Ti_{50}Ni_{25}Cu_{25}$ alloy crystallizes through a single stage polymorphic reaction forming a facted Ti_2NiCu phase. Ti_2NiCu phase was found to have a cubic lattice with a lattice parameter $a = 0.3047$ nm. The lattice parameter is very close to that of the Pm 3m cubic NiTi phase that allows us to suppose that this phase is a solid solution of Cu in NiTi phase.

At long time of holding at elevated temperature γ CuTi phase of plate-shaped morphology precipitates from the Ti_2NiCu one and composition of the above-mentioned ternary phase changes. After such an annealing Ti_2NiCu phase is depleted in Ti and Cu compare to the composition of the as-crystallized Ti_2NiCu phase measured after the single exothermic reaction. $TiNi_{0.8}Cu_{0.2}$ phase having a tetragonal structure of $a = 0.3108$ nm and $c = 0.5887$ nm precipitates at higher temperature. An unidentified phase(s) has been also observed.

High average value of Avrami exponent of 5.5 at the range from 702 to 709 K suggests nucleation of Ti_2NiCu with an increasing nucleation rate. The activation energy for the crystallization of the amorphous phase is 306 kJ/mol. Ti_2NiCu phase shows a relatively high thermal stability against decomposition.

References

1. T. ZHANG and A. INOUE, *Mater. Trans. JIM* **39** (1998) 1001.
2. T. ZHANG, A. INOUE and T. MASUMOTO, *Mater Sci. Eng.* **A181/182** (1994) 1423.
3. H. E. KISSINGER, *J. Res. National. Bureau Stand.* **57** (1956) 217.
4. J. W. CHRISTIAN, "The Theory of Transformations in Metals and Alloys" (Pergamon Press Ltd., Oxford, 1975) p. 540.
5. K. KARLSSON, *J. Inst. Met.* **79** (1951) 391.
6. Y. SHUGO and T. HONMA, *Tohoku Daigaku Senko Seiren Kenkyusho Iho* (in Japanese) **43** (1987) 117.
7. M. BUCHWITZ, R. ADLWARTH-DIEDALL and P. L. RYDER, *Acta Metall. Mater.* **41** (1993) 1885.
8. P. VILLARS, A. PRINCE and H. OKAMOTO, "Ternary Alloy Phase Diagrams" (ASM International, Ohio, 1995) p. 3744.

Received 6 May
and accepted 19 August 1999